Statics Analysis and Optimization Design for a Fixed-Guided Beam Flexure

Ngoc Thoai TRAN[1], *Thanh-Phong DAO*[2,3,*]

[1]Faculty of Mechanical Engineering, Industrial University of Ho Chi Minh City, Ho Chi Minh City, Vietnam
[2]Division of Computational Mechatronics, Institute for Computational Science, Ton Duc Thang University, Ho Chi Minh City, Vietnam
[3]Faculty of Electrical and Electronics Engineering, Ton Duc Thang University, Ho Chi Minh City, Vietnam

*Corresponding Author: Thanh-Phong DAO (Email: daothanhphong@tdtu.edu.vn)
(Received: 24-Dec-2019; accepted: 26-Feb-2020; published: 30-Jun-2020)
DOI: http://dx.doi.org/10.25073/jaec.202041.276

Abstract. *The ratchet mechanism has been used to ensure moving in one direction of rotation, i.e. either clockwise or counter-clockwise. This mechanism is designed based on fixed-guided beam flexures to reduce friction, and improves accuracy compared to the traditional mechanism. This paper presents a static analysis and parameter optimization for the fixed-guided beam flexures via using the pseudo-rigid-body model and a fmincon algorithm. The Finite Element Method (FEM) of the fixed-guided beam also has been used to verify the maximum stress and the $x-$direction displacement. Modified pseudo-rigid-body model (M-PRBM) is also applied to significantly enhance the accuracy of the maximum stress value. The results show that the averaged errors of maximum stress between M-PRBM and FEM are 3.48% for aluminum, and less than 10.9% for titanium, carbon steel, and alloy steel. From the obtained results, the M-PRBM is good for prototype design and fabrication of ratchet mechanism in the future.*

Keywords

Ratchet mechanism, compliant mechanism, constrained optimization, pseudo-rigid-body model, fixed-guided beam.

1. Introduction

Compliant mechanism (CM) [1] has received much attention in the last two decades because of their advantages such as free friction, no lubricant, reduced maintenance, increased precision, and lightweight compared with a conventionally kinematic mechanism. Ratchet mechanism is a common application of CM. This mechanism allows continuous linear or rotary motion in only one direction while preventing motion in the opposite direction. Ratchet mechanisms are widely used in machinery and tools such as a safety and accuracy device. This mechanism uses two fixed-guided compliant beams to store energy when it is subjected to force [2]. The fixed-guided compliant beams also used in the gripper mechanism [3]. Two common approaches to design and analysis for this mechanism includes pseudo-rigid-body model (PRBM) [4]-[6] and finite element analysis (FEA) [7, 8]. But, the error of the maximum stress value between PRBM and FEA is so large. To increase accuracy, a modified pseudo-rigid-body model (M-PRBM) approach is applied for fixed-guided bistable compliant mechanisms [9]. Kennedy et al. [10] designed a ratchet mechanism by using two fixed-pinned compliant beams and two fixed-guided compliant beams. Although the ratchet mechanism was well de-

signed; however, this study has not optimized the parameters of fixed-guided beam flexures to enhance its performances yet. Recent studies have conducted an optimization design for several compliant mechanisms in various applications, e.g. solar panel [11], a micro-displacement sensor for compliant micro-gripper [12]-[14], or compliant joint for camera positioning system of nanoindentation tester [15, 16]. However, an optimization design for the ratchet mechanism has been poorly studied.

In this paper, we introduce an overview of the structural design process of fixed-guided beam flexures. Unlike previous studies, we optimize geometric parameters to improve the performances of the flexures. Then, we have conducted effects of various materials and dimensions on the performances through numerical analysis. The goal of this article is to modeling static performances of the ratchet mechanism. And then, this study conducts an optimization design to enhance its performances. Aluminum material is recommended for this mechanism because of a good ratio of seven between the yield strength and Young's modulus. Other materials are further investigated as a potential of CM to expand the working ability of this mechanism. The maximum stress and the $x-$direction displacement are calculated by PRBM and finite element method (FEM). After that, M-PRBM of fixed-guided mechanisms is proposed to increase maximum stress accuracy.

2. Mechanism design

2.1. Selection of configuration

In this paper, the ratchet mechanism is designed by using beam flexures. The structure of beam flexures is designed with three parts as follows: i) The base is fixed to the ground through-bolted joints of two holes with 6 mm in diameter. ii) The body consists of fixed-guided beams arranged perpendicular to the base to support the top beam and store energy when the top beam is subjected to force in $x-$direction. Afterward, it moves to its original position when the top beam is no longer subject to force. iii) The top part is a horizontal beam that is responsible for ensuring the movement of the ratchet.

Three different configurations, which have various numbers of vertical beams, are adopted to numerically analyze the horizontal ($x-$direction) displacement and stress, seen in Figs. 1(a), 1(b) [10], and 1(c) [17]. These configurations may be used to design compliant with a high-precisions mechanism for safety and the arm device. By using ANSYS 18.1 software, the simulation results found that the displacement of one beam is highest, followed by two beams, and the displacement of three beams is lowest, as shown in Fig. 2, respectively.

Another important aspect of the ratchet mechanism is how to improve its positioning precision. This can be achieved by decreasing an undesired motion, called as parasitic error. In the ratchet mechanism, the y-direction displacement is the so-called parasitical displacement [1]. A similar simulation is conducted for three cases in Fig. 2. As depicted in Fig. 3, the results indicated that the parasitic displacement of the first configuration in Fig. 3(a) is largest, followed by the second configuration, and the last one has the smallest value of parasitic error. Besides, if this error is large, then the ratchet mechanism could not work efficiently. The configurations in Figs. 1(a) and 1(c) ensure their working requirement. So, these mechanisms meet the designed requirements. The configuration in Fig. 1(c) has the working space, and its manufacturing process has a higher cost than that in Fig. 1(b). However, these factors are not important, and so the design of that in Fig. 1(b) should be used for the ratchet mechanism. The description of its features is presented below.

2.2. Mechanism design

A mechanism, as shown in Fig. 4, consists of two vertical parallel fixed-guided beams (i.e. the beam ends link to a fixed base, and the others connect to the horizontal top beam). The dimensions of the fixed base and the horizontal top beam are the constant values given in Tab. 1. They are referenced in [10] with a scale to match the mechanism size. Since the horizon-

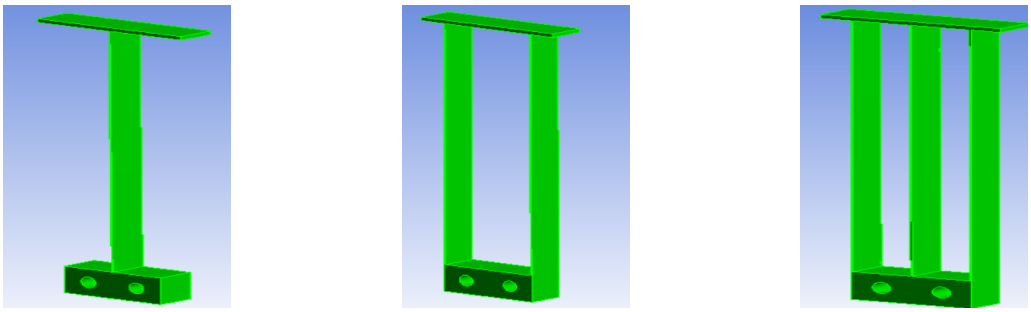

(a) (b) (c)

Fig. 1: Three different configurations of fixed-guided beam flexure: (a) one beam; (b) two parallel beams; (c) three parallel beams.

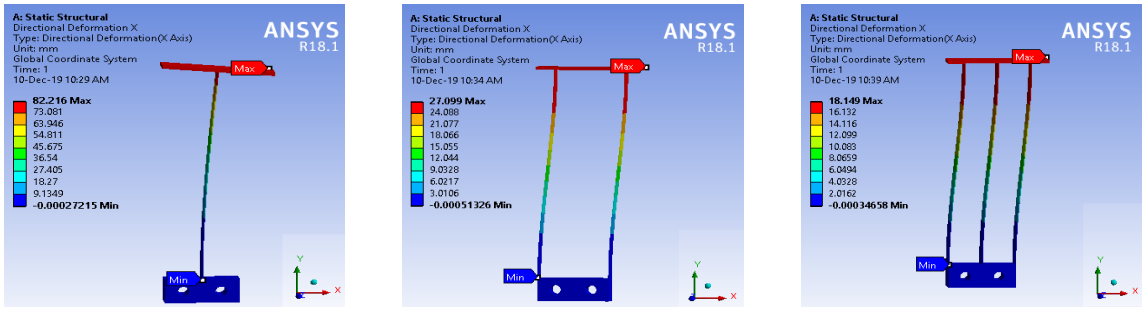

(a) (b) (c)

Fig. 2: The simulation results of the $x-$direction displacements: (a) one beam; (b) two parallel beams; (c) three parallel beams.

tal top beam is exerted the $x-$direction force F, and it will be displaced in the $x-$direction. The two vertical fixed-guided beams will be bent, and they store elastic energy. Thanks to this energy, the top beam is back the original location when the force F is released. The process will be repeated with the constant value of the force F.

The two fixed-guided beams not only must be designed to ensure the domestic machinability but also depend on the requirement of the compliant mechanism [1]. Therefore, the beam height, h, should be varied between 0.4 mm and 0.6 mm. The fabrication method for the prototype of mechanism can be used such as wire electric discharge matching. The two fixed-guided beams not only must be designed to ensure the domestic machinability but also depend on the requirement of the compliant mechanism. Domestic machining by the EDM method is 0.4 mm in diameter. Therefore, the beam height, h, should be varied between 0.4 mm and 0.6 mm.

Tab. 1: The design values are constant of the mechanism

Variable	Value (mm)	Description
H_{top}	2	Height of the top beam
h_{ground}	15	Height of the ground link
B	40	Width of the ground link
r	3	Radius of the fixed hole
L_{top}	60	Length of the top beam

According to the theory of elastic deformation [18] based on the Kirchhoff hypothesis, the thin plate requires the ratio between the width and thickness must be greater than 30.

The material used in the whole mechanism is AL 7075-T6 [15]. It has a good ratio of seven be-

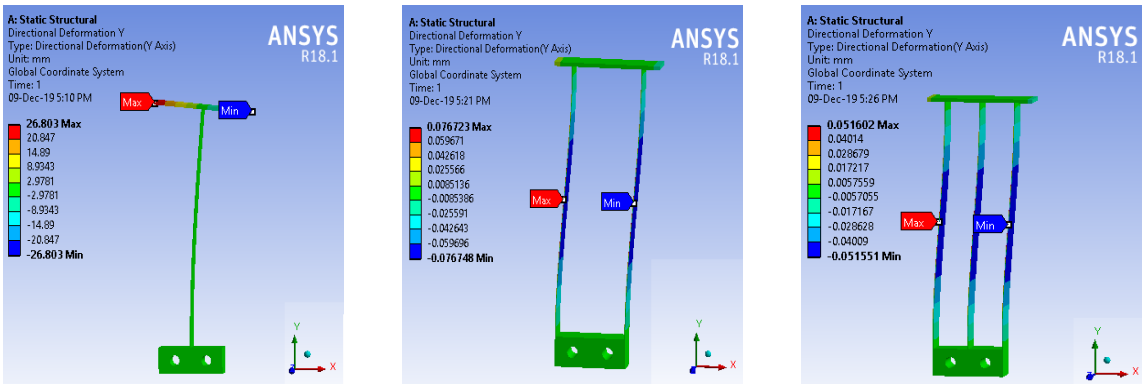

(a) (b) (c)

Fig. 3: The simulation results of the $x-$direction displacements: (a) one beam; (b) two parallel beams; (c) three parallel beams.

Tab. 2: Parameters of AL 7075-T6 material

Variable	Value	Description
E	71700 (MPa)	Young's modulus
d	2770 (kg/m^3)	Density
v	0.33	Poisson's ratio
S_Y	503 (MPa)	Tensile yield strength

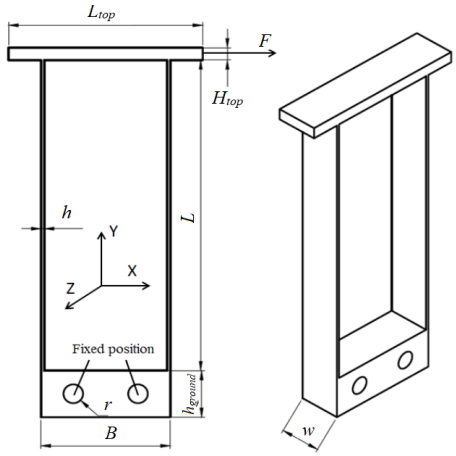

Fig. 4: Structure of two parallel fixed-guided beams (mm).

tween the yield strength and Young's modulus. This value is ideal for compliant mechanisms [1]. The materials with the highest strength-to-modulus ratio will allow a larger deflection before failure. Good materials have a high ratio. The parameters of this material are given in Tab. 2.

The structure of the whole mechanism should be a block as seen in Fig. 4, (i.e. there are no joints between the beams). The dimensions of two fixed-guided beams are designed by applying the pseudo-rigid-body model (PRBM) theory [1], and are optimized by using the Optimization tool of the Matlab software [19]. These will be presented in the next section.

3. Static analysis and parameter optimization

3.1. Pseudo-rigid-body model

In this section, the fixed-guided mechanism is analyzed though PRBM, as shown in Fig. 5. This method has been proposed by Howell [1], and has been applied to other mechanisms [4, 9]. This model is particularly useful for the large deflection analysis. Two fixed-guided beams used in this mechanism have no original curvature, and the moment is zero at the mid-point of the beam.

Tab. 3: Design parameters of fixed-guided beam.

Variable	Value	Description
F	3 (N)	Horizontal force applied at the end of the top beam
K_Θ	2.67617	Stiffness coefficient
γ	0.8517	Characteristic radius factor
Θ	13^0	Pseudo-rigid-body angle
SF	1.5	Safety factor

The design parameters of the two beams are given in Tab. 3. The values of $K_\Theta, \gamma\Theta_{\max}$ are referenced in [1]. The safety factor, $SF = 1.5$ [20] for well-known materials, under reasonably constant environmental conditions, subjected to loads and stresses that can be determined readily. The symbols indicated the width, height,

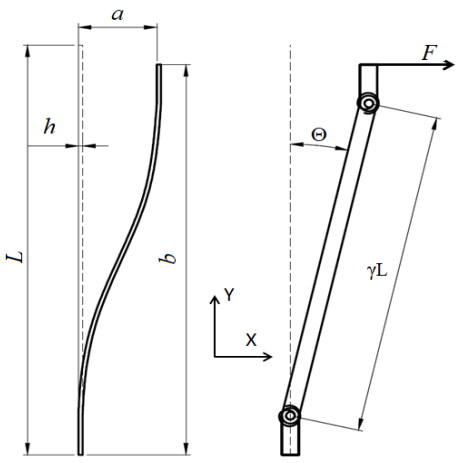

Fig. 5: Pseudo-rigid-body model of fixed-guided beam (mm).

and length of the fixed-guided beam are given as w, h and L, respectively. Those dimensions need to be designed beams.

The x-direction displacement of the beam is given by Howell [1] as

$$\delta_x = a = \gamma L \sin\Theta. \tag{1}$$

The $y-$direction displacement of the beam is addressed as

$$\begin{aligned}\delta_y &= L - b \\ &= L - L\left(1 - \gamma\left(1 - \cos\Theta\right)\right) \\ &= \gamma L\left(1 - \cos\Theta\right),\end{aligned} \tag{2}$$

where,

$$b = L\left(1 - \gamma\left(1 - cos\Theta\right)\right). \tag{3}$$

The spring constant of the beam is computed by

$$K = 2\gamma K_\Theta \frac{EI}{L}, \tag{4}$$

where, the moment of inertia of the beam

$$I = \frac{wh^3}{12}. \tag{5}$$

Using the virtual work principle, force F causes the deformation of the beam to be measured by an equation

$$F = \frac{4K\Theta}{\gamma L cos\Theta}. \tag{6}$$

Maximum stress at the end of the beam is

$$\sigma_{max} = \frac{Fbc}{2I} = \frac{Fbh}{4I}, \tag{7}$$

where, c is distance from neutral shaft to outer surface of beam

$$c = \frac{h}{2}. \tag{8}$$

Permissible stress is calculated by

$$[\sigma_u] = \frac{S_Y}{SF}. \tag{9}$$

From Eqs. (4)-(6) equations, the length of beam flexure is computed as

$$L = \frac{4K\Theta}{\gamma F cos\Theta} = \frac{2}{3}\frac{\Theta K_\Theta E}{LF cos\Theta} wh^3, \tag{10}$$

or,

$$L = \sqrt{\frac{2}{3}\frac{\Theta K_\Theta E}{F cos\Theta}}\sqrt{wh^3}. \tag{11}$$

From (1) and (11) equations. The $x-$direction displacement of the beam

$$\delta_x = \gamma \sin\Theta\sqrt{\frac{2}{3}\frac{\Theta K_\Theta E}{F cos\Theta}}\sqrt{wh^3} = p\sqrt{wh^3}, \tag{12}$$

where, p is displacement coefficient in $x-$directions

$$p = \gamma \sin\Theta \sqrt{\frac{2}{3}\frac{\Theta K_\Theta E}{F cos\Theta}}. \quad (13)$$

From Eqs. (3), (5), and (7), the stress is found as

$$\sigma_{max} = \frac{Fbh}{4I} = \frac{Fh}{4} L\left(1-\gamma\left(1-cos\Theta\right)\right)\frac{12}{wh^3}. \quad (14)$$

Maximum stress at the end of the beam

$$\sigma_{max} = \left(1-\gamma\left(1-cos\Theta\right)\right)\sqrt{\frac{6F\Theta K_\Theta E}{cos\Theta}}\frac{1}{\sqrt{wh}} = q\frac{1}{\sqrt{wh}}, \quad (15)$$

where, q is coefficient of maximum stress

$$q = \left(1-\gamma\left(1-cos\Theta\right)\right)\sqrt{\frac{6F\Theta K_\Theta E}{cos\Theta}}. \quad (16)$$

3.2. Optimization design

The optimal design [19] is always mentioned in structural design problems to ensure the minimum use of materials to minimize the production cost and maximize the performance of the mechanism. Design variables need to be optimized including the width, height, and length of the fixed-guided beam. To achieve these optimal values, the problem is set up as follows:

- Design variables: The length of the fixed-guided beam is calculated using equation (11).
- Design vector [$\mathbb{X}$]:

$$[\mathbf{X}] = [x_1, x_2]^T = [w, h]^T. \quad (17)$$

- Objective function: The objective function is set based on the work requirement of mechanism. The horizontal $x-$direction displacement reaches the desired value. Therefore, based on equation (12), the objective function in this problem is given

$$F(X) = p\sqrt{x_1 x_2^3} \rightarrow \max. \quad (18)$$

- Equality constraint: The ratio between displacements in the y and the $x-$directions

$$h(x): \frac{\delta_y}{\delta_x} = \frac{\gamma L\left(1-\cos\Theta\right)}{\gamma L sin\Theta} = \frac{\left(1-\cos\Theta\right)}{\sin\Theta} = 0.114. \quad (19)$$

- Inequality constraints: To ensure the working ability of the mechanism, the maximum stress of the beam σ_{max} will be not exceed the permissible stress $[\sigma_u]$. Combining equations (9) and (15), we obtain

$$g_1(x): q\frac{1}{\sqrt{x_1 x_2}} \leqslant \frac{S_Y}{SF} = \frac{503}{1.5} = 335, \quad (20)$$

or,

$$g_1(x): q\frac{1}{\sqrt{x_1 x_2}} - 335 \leqslant 0. \quad (21)$$

Besides, in the mechanism design, the ratio between the width and height is given

$$g_2(x): \frac{x_1}{x_2} \geqslant 30, \quad (22)$$

or,

$$g_2(x): -\frac{x_1}{x_2} + 30 \leqslant 0. \quad (23)$$

The displacement of the y-direction of the beam is the parasitical displacement. Therefore, it needs to have a constraint not to affect the performance of the function of the mechanism

$$\mathrm{g}_3(x): \gamma\left(1-\cos\Theta\right)\sqrt{\frac{2}{3}\frac{\Theta K_\Theta E}{F\cos\Theta}}\sqrt{x_1 x_2^3} \leqslant 3, \quad (24)$$

or,

$$\mathrm{g}_3(x): k\sqrt{x_1 x_2^3} - 3 \leqslant 0. \quad (25)$$

where, k is displacement coefficient in $y-$direction

$$k = \gamma\left(1-\cos\Theta\right)\sqrt{\frac{2}{3}\frac{\Theta K_\Theta E}{F\cos\Theta}}. \quad (26)$$

Tab. 4: Comparison of three different meshing methods.

	PRBM	Three different meshes					
		Automatic Meshing		Refinement Meshing		Sizing Meshing	
		FEM	Error %	FEM	Error %	FEM	Error %
Displacement in the x-direction (mm)	26.1431	25.641	1.92	27.099	3.66	22.236	14.95
Maximum stress (N/mm^2)	320.326	168.75	47.32	182.45	43.04	123.84	61.34
Quality (Skewness)		0.52 (Good)		0.72 (Fair)		0.77 (Poor)	
Statistics		Nodes 3867	Elements 588	Nodes 27744	Elements 13054	Nodes 1394	Elements 232

Tab. 5: Comparison of three different meshing methods.

h (mm)	w(mm)	Maximum stress (N/mm^2)					
		M-PRBM	FEM	Error %	PRBM	FEM	Error %
0.4	12	210.94	214.14	1.52	400.41	214.14	46.52
	13	202.67	211.71	4.46	384.71	211.71	44.97
	14	195.29	197.68	1.22	370.70	197.68	46.67
	15	188.67	193.31	2.46	358.13	193.31	46.02
0.5	12	188.67	196.62	4.21	358.13	196.62	45.10
	13	181.27	191.65	5.73	344.09	191.65	44.30
	14	174.68	182.01	4.20	331.58	182.01	45.11
	15	168.75	168.75	0.00	320.32	168.75	47.32
0.6	12	172.23	177.93	3.31	326.93	177.93	45.58
	13	165.48	174.61	5.52	314.11	174.61	44.41
	14	159.46	165.81	3.98	302.69	165.81	45.22
	15	154.05	162.01	5.17	292.42	162.01	44.60

Tab. 6: The parameters of four materials using in mechanism.

Material	Density ρ (kg/m^3)	Young's modulus (E) (MPa)	Poisson's ratio (ν)	Tensile yield strength S_Y (MPa)	$\frac{S_Y}{E} \times 1000$
AL 7075-T6	2770	71700	0.33	503	7
Titanium Alloys Ti-13 heat treated	4400	113800	0.34	1170	10
Stainless steel 17-7TH 1050	7640	202700	0.28	1034	5
Carbon steel 4130 Q&T 800	7800	206800	0.28	1190	6

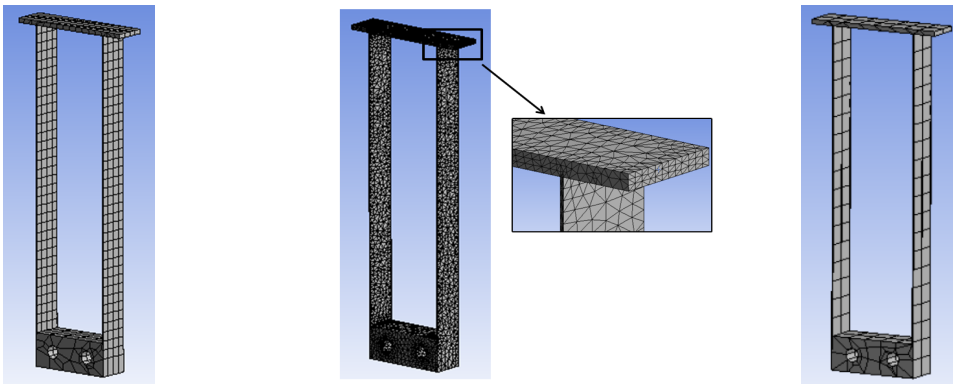

(a) (b) (c)

Fig. 6: Different meshes model of mechanism: (a) automatic mesh; (b) refinement mesh; (c) sizing mesh.

- Design spaces:

$$\begin{aligned} 12 \leqslant x_1 \leqslant 15 \\ 0.4 \leqslant x_2 \leqslant 0.6 \\ 80 \leqslant x_3 \leqslant 300 \end{aligned} \tag{27}$$

Finally, we use the Matlab R2016b software to optimize the objective function with the "fmincon" function (i.e. objective function is now $-f(x)$). The optimal results are obtained:

$$[\mathbf{X}] = [x_1, x_2]^T = [15, 0.5]^T.$$

So, the optimal sizes are used to design the mechanism as

$$w = 15 \text{ mm}; h = 0.5 \text{ mm}; L = 136 \text{ mm}.$$

3.3. Finite element method

FEM is used to verify the deviations of the PRBM presented in the previous section. This method uses the constant parameters in Tab. 1 with the material used is AL 7075-T6. The ANSYS 18.1 software used in this method helps to visually illustrate the movement of the device after applying the force F in the $x-$direction.

Meshing method: In FEM, the mesh is very important that affects the simulation results. In FEM we use three common types of mesh in Fig. 6 such as meshing automatic method, refinement coupled with an automatic method, and sizing method. Automatic meshing reduces time but the results of the mesh may not converge, resulting in less accurate calculations. For better calculation results, refinement mesh can be used. However, in some cases such as a simple structure or a difficult mesh to split, the use of refinement mesh is not necessary. Sizing mesh based on size to mesh should take time to find optimal results. To assess the quality of the mesh, skewness standards are used.

The optimal size values are simulated with three different mesh types. The simulation results of displacements in the $x-$direction and maximum stresses will be compared with those of PRBM, seen in Tab. 4. Besides, skewness standard, number of elements and number of nodes are used to assess the quality of the meshes. With the results shown in Tab. 4, the sizing mesh is not used in simulation because Skewness value has pool and error of displacements in the $x-$direction and maximum stresses are large. The displacements error of automatic mesh and refinement mesh are small so FEM is suitable for calculation with this value. Opposite, the maximum stress errors of above two methods are large. Among the above meshes, the Skewness standard of automatic mesh has the best value. So, the automatic mesh is only the best fit in this design. In addition, the errors between the PRBM and FEM in case of stress is very large. Therefore, the PRBM is almost suitable to model the displacement but this method is failed to analyze the stress.

According to the simulation results in Fig. 3(b), the value of parasitical displacement is very small. So, it will not affect the operation of the mechanism, and is neglected.

3.4. Modified Pseudo-rigid-body model (M-PRBM)

From the FEM results obtained, the averaged errors of displacements in the $x-$direction are less than 7%. Those of the maximum stresses are greater than 50%. There is a large error of max. Stress between the FEA simulations and the PRBM using for thin bar elastic deformation. This may be explained by the following reasons: 1) the compliant mechanisms are often used in structures that require small displacements and 2) the limitation of the PRBM model, which replaces the links between beams by the torsion springs, should ensure the accuracy of deformation in the $x-$direction only. In order to obtain the accuracy of the maximum stress value in the calculation, the coefficient α is added as,

$$\alpha = \frac{\sigma_{tinh\ toan}}{\sigma_{mo\ phong}} = \frac{320.326}{168.75} = 1.8982, \qquad (28)$$

Where α is the conversion coefficient of stress. Thus, to calculate the maximum stress values when using the PRBM model, we use the following equation:

$$\sigma_{max} = \frac{1}{\alpha}\left(1 - \gamma\left(1 - \cos\Theta\right)\right)\sqrt{\frac{6F\Theta K_\Theta E}{\cos\Theta}}\frac{1}{\sqrt{wh}}. \qquad (29)$$

The calculated M-PRBM results after using the coefficients $\alpha = 1.8982$ and their errors with those of FEM ones are presented in Tab. 5.

With the results shown in Tab. 5, the difference in the maximum stress values between the M-PRBM and FEM with the height $h = 0.4$ mm is less than 5%. That of $h = 0.5$ mm and 0.6 mm is less than 6% in Fig. 7. Thus, the value of deviation between the PRBM and FEM depends heavily on the height value. This is entirely consistent with the theory of compliant mechanism. In the viewpoint of machinability, the result of the displacement in the $x-$direction and the maximum stress will have high accuracy with the small value of h. However, according to the domestic process, the $h-$value can only be

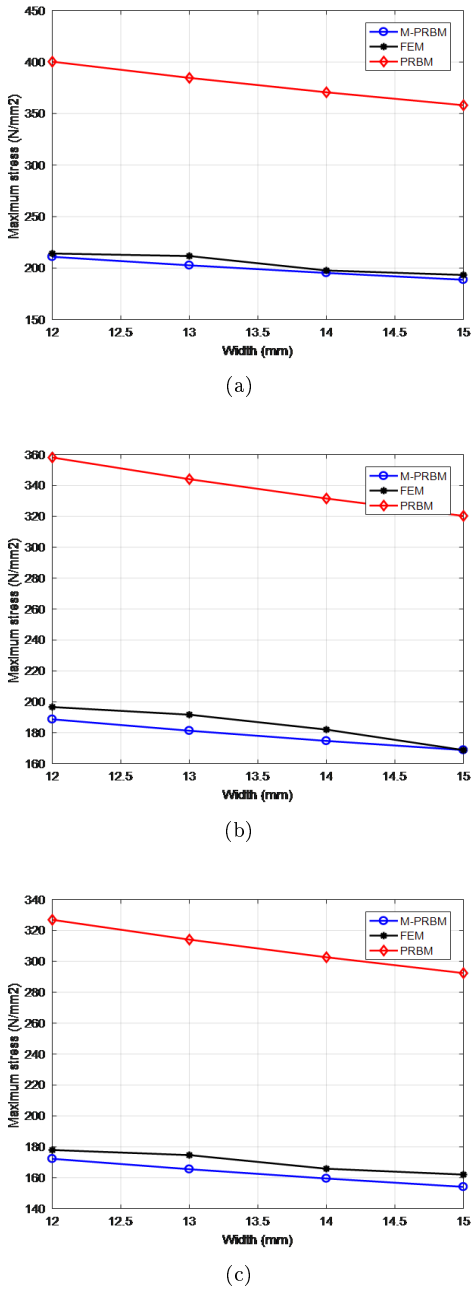

Fig. 7: Distribution of maximum stress against the beam width of different methods: M-PRBM, FEM, and PRBM. (a) $h = 0.4$ mm; (b) $h = 0.5$ mm; (c) $h = 0.6$ mm.

processed with a minimum of 0.4 mm when the width is greater than 12 mm. Therefore, in the next section, the min. value of h from 0.4 mm is used to compare those between M-PRBM and FEM methods with different materials.

4. Influence of materials and configurations to maximum stress and $x-$direction displacement

In this section, the different materials and configurations are examined in order to enhance the applicability of the mechanism. The parameter of four different materials is shown in Tab. 6. The good materials must have the ratio between the yield strength and Young's modulus more than 5.

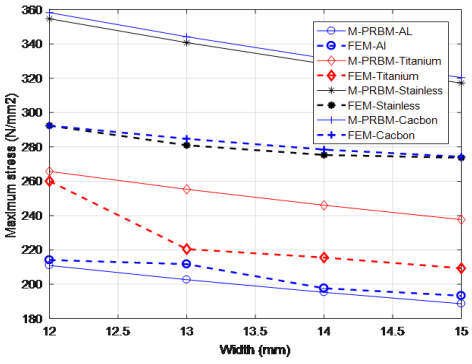

Fig. 8: Distribution of maximum stress against the beam width, $h = 0.4$ mm.

Case 1: $h = 0.4$

Based on design space in Eq. (27), the value of L is calculated by Eq. (11) depending on the 2 variables h and w. Calculation results for $h = 0.4$ mm are presented in Tab. 7, and plotted in Fig. 8 and Fig. 9. Maximum stress distributions of four different materials are plotted against the beam width, seen in Fig. 8. They are calculated by the M-PRBM and FEM. By increasing the beam width, all of the stresses gradually decrease (i.e. the maximum stress is inversely proportional to the increase of the beam width). The maximum stresses of carbon and stainless steels are 358 N/mm^2 and 354 N/mm^2, respectively. Those of non-steel such as titanium and aluminum are 266 N/mm^2 and 214 N/mm^2, respectively. The maximum stresses of the carbon and stainless steels are approximate values, and are higher than those of the titanium and aluminum. The averaged errors between the M-PRBM and FEM are 15.69%, 17.08%, 10.02% and 2.42% for the carbon steel, stainless steel, titanium, and aluminum, respectively. There are large differences between two methods for the carbon steel, stainless steel, and titanium while there is a good agreement between them for the aluminum. This may be explained by the elastic modulus of aluminum smaller than the other materials. It is noted that the elastic modulus affects the calculation of the maximum stress. When the modulus E value of each material is changed, L value also changes according to equation (11). This results in that of the aluminum obtain the smallest values.

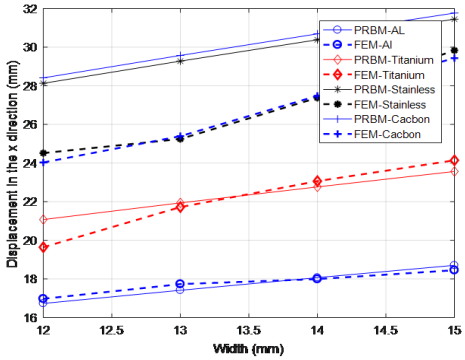

Fig. 9: Distribution of displacement in the $x-$direction against the beam width, $h = 0.4$ mm.

Calculated displacements in the $x-$direction profile of four different materials are drawn against the beam width, seen in Fig. 9. They are computed by the PRBM and FEM methods. By growing the beam width, all of the displacements considerably gradual rise (i.e. the displacements in the $x-$direction is proportional to the increase of the beam width). The maximum displacements in the $x-$direction of carbon and stainless steels are 31.77 mm and 31.45 mm, respectively. Those of non-steel such as titanium

Tab. 7: Comparing the difference of maximum stress and displacement in the $x-$direction values, $h = 0.4$ mm.

Material	w (mm)	Maximum stress (N/mm^2)			Displacement in the $x-$direction (mm)		
		M-PRBM	FEM	Error %	PRBM	FEM	Error %
AL 7075-T6	12	210.94	214.14	1.52	16.732	16.974	1.45
	13	202.67	211.71	4.46	17.415	17.734	1.83
	14	195.29	197.68	1.22	18.072	17.994	0.43
	15	188.67	193.31	2.46	18.706	18.454	1.35
Titanium Alloys Ti-13 heat treated	12	265.75	260.08	2.13	21.079	19.644	6.81
	13	255.32	220.48	13.65	21.940	21.722	0.99
	14	246.03	215.59	12.37	22.768	23.067	1.31
	15	237.69	209.32	11.94	23.567	24.145	2.45
Stainless steel 17-7TH 1050	12	354.67	292.41	18.38	28.132	24.52	13.71
	13	340.76	280.99	18.36	29.281	25.249	14.63
	14	328.36	275.33	16.99	30.386	27.381	10.79
	15	317.23	273.71	14.58	31.453	29.837	6.08
Carbon steel 4130 Q&T 800	12	358.24	292.41	17.55	28.415	24.033	14.57
	13	344.19	284.75	16.44	29.576	25.395	13.27
	14	331.67	278.46	15.20	30.692	27.484	9.55
	15	320.42	274.24	13.55	31.769	29.435	6.42

and aluminum are 24.15 mm and 18.71 mm, respectively. The maximum displacements of the carbon and stainless steels are approximate values, and are higher than those of the titanium and aluminum. The averaged errors between the PRBM and FEM are 11.30%, 11.56%, 2.89% and 1.27% for carbon steel, stainless steel, titanium, and aluminum, respectively. There are large differences between the two aforementioned methods for carbon steel, stainless steel. There are good agreements between them for titanium and aluminum. Similar to the calculated results of the maximum stresses, the elastic modulus of aluminum is smaller than that of the other materials. This leads to the displacement of the aluminum obtains the smallest values.

Case 2: $h = 0.5$

Similar to the calculated method of the $h = 0.4$ mm. Calculation results for $h = 0.5$ mm are presented in Tab. 8, and plotted in Fig. 10 and Fig. 11.

The data in Fig. 10 shows that maximum stress distributions of four different materials are plotted against the beam width. Similar to the calculated results of the maximum stresses show in Fig. 8. All of the stresses also decrease when the beam width increase. The averaged errors of the carbon steel, stainless steel, titanium, and aluminum are 16.44%, 12.02%, 14.02%, and 3.54%, respectively. The maximum stresses of those are 320 N/mm^2, 317 N/mm^2, 238 N/mm^2, and 197 N/mm^2, respectively. The maximum stresses of the titanium and aluminum lower than of the carbon and stainless steel. The carbon steel, stainless steel, and titanium have large averaged errors while the aluminum is nearly accuracy. This may be explained similarly to the calculated results of the maximum stresses with h =0.4 mm. The data in Fig. 11 shows that calculated displacements in the $x-$direction profile of four different materials are drawn against the beam width. The maximum displacements in the $x-$direction of titanium and aluminum are 32.94 mm and 26.14 mm, respectively while carbon and stainless steels of this value are 44.4 mm and 43.96 mm, respectively. The averaged errors of the carbon steel, stainless steel, titanium and aluminum between the PRBM and FEM are 14.56%, 15.21%, 4.83%, and 2.96%, respectively. Similarly, as Fig. 9, the displacement of the aluminum obtains the smallest values.

Case 3: $h = 0.6$

Tab. 8: Comparing the difference of maximum stress and displacement in the x-direction values, $h = 0.5$ mm.

Material	w(mm)	Maximum stress (N/mm^2)			Displacement in the $x-$direction (mm)		
		M-PRBM	FEM	Error %	PRBM	FEM	Error %
AL 7075-T6	12	188.67	196.62	4.21	23.383	24.548	4.98
	13	181.27	191.65	5.73	24.338	25.424	4.46
	14	174.68	182.01	4.20	25.257	25.746	1.94
	15	168.75	168.75	0.00	26.143	26.007	0.52
Titanium Alloys Ti-13 heat treated	12	237.69	198.07	16.67	29.459	26.274	10.81
	13	228.37	192.45	15.73	30.662	28.747	6.25
	14	220.06	191.09	13.16	31.819	31.195	1.96
	15	212.6	190.23	10.52	32.936	32.845	0.28
Stainless steel 17-7TH 1050	12	317.23	275.53	13.15	39.316	34.545	12.14
	13	304.784	251.85	17.37	40.921	34.696	15.21
	14	293.7	242.19	17.54	42.466	35.573	16.23
	15	283.74	230.53	18.75	43.957	36.379	17.24
Carbon steel 4130 Q&T 800	12	320.42	276.25	13.79	39.712	34.199	13.88
	13	307.85	257.39	16.39	41.333	34.85	15.68
	14	296.65	241.38	18.63	42.893	35.91	16.28
	15	286.59	238.04	16.94	44.399	38.894	12.40

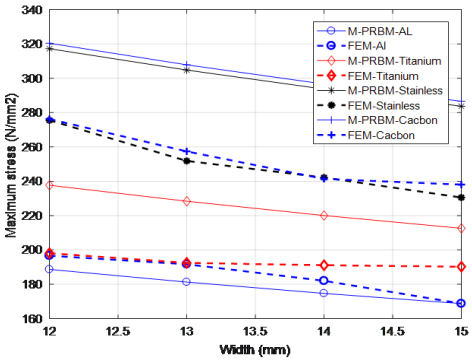

Fig. 10: Distribution of maximum stress against the beam width, $h = 0.5$ mm.

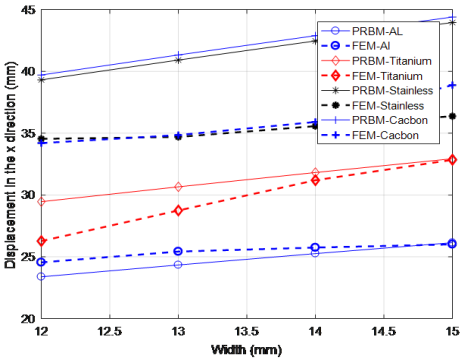

Fig. 11: Distribution of displacement in the $x-$direction against the beam width, $h = 0.5$ mm.

Calculation results for $h = 0.6$ mm are presented in Tab. 9, and plotted in Fig. 12 and Fig. 13.

Maximum stress results drawn in Fig. 12 can be compared with the data in Fig. 8. The averaged error of titanium is 13.84%, and of the carbon steel, stainless steel, and aluminum are 4.96%, 4.56%, and 4.5%, respectively. There is a large difference between the PRBM and FEM for the titanium while there is a good agreement between them for the other materials. The maximum stresses of those are 292.5 N/mm^2 and 289.59 N/mm^2, 216.98 N/mm^2 and 177.93 N/mm^2, respectively. Figure 13 is drawn displacements in the x-direction of four materials such as carbon steel, stainless steel, and aluminum and titanium. Those values are calculated by the PRBM and FEM methods. The maximum displacements in the $x-$direction of carbon and stainless steel are 61.49 mm and 60.35 mm, respectively. Those of non-steel such as titanium and aluminum are 43.3 mm and 35.5 mm, respectively. The maximum displacements

Tab. 9: Comparing the difference of maximum stress and displacement in the x-direction values, $h = 0.6$ mm.

Material	w(mm)	Maximum stress (N/mm^2)			Displacement in the $x-$direction (mm)		
		M-PRBM	FEM	Error %	PRBM	FEM	Error %
AL 7075-T6	12	172.23	177.93	3.31	30.738	31.467	2.37
	13	165.48	174.61	5.52	31.993	31.862	0.41
	14	159.46	165.81	3.98	33.201	34.632	4.31
	15	154.05	162.01	5.17	34.366	35.498	3.29
Titanium Alloys Ti-13 heat treated	12	216.98	191.45	11.77	38.724	37.114	4.16
	13	208.47	181.42	12.98	40.306	38.011	5.69
	14	200.89	170.78	14.99	41.827	38.429	8.12
	15	194.08	163.81	15.60	43.295	39.681	8.35
Stainless steel 17-7TH 1050	12	289.59	274.37	5.26	51.682	54.745	5.93
	13	278.23	262.11	5.79	53.792	56.392	4.83
	14	268.11	260.05	3.01	55.823	59.21	6.07
	15	259.02	248.2	4.18	57.782	60.348	4.44
Carbon steel 4130 Q&T 800	12	292.5	278.53	4.78	52.202	55.87	7.03
	13	281.03	266.28	5.25	54.334	57.863	6.50
	14	270.81	252.42	6.79	56.385	61.355	8.81
	15	261.62	253.74	3.01	58.364	61.486	5.35

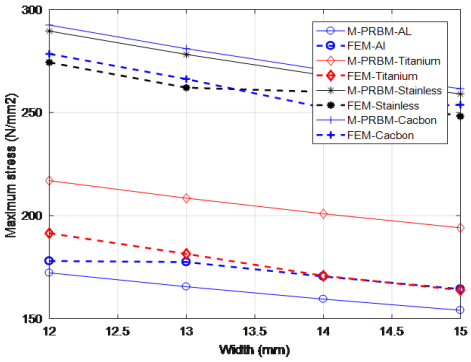

Fig. 12: Distribution of maximum stress against the beam width, $h = 0.6$ mm.

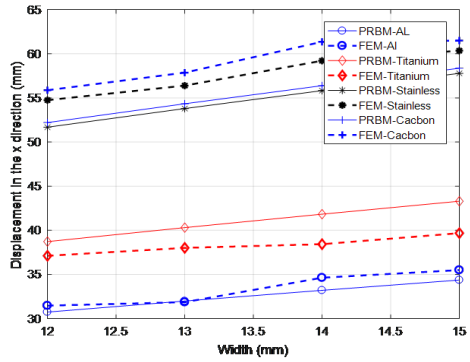

Fig. 13: Distribution of displacement in the $x-$direction against the beam width, $h = 0.6$ mm.

of the titanium and aluminum are approximate values and less than the carbon and stainless steels. The averaged errors between the PRBM and FEM are 6.92%, 5.32%, 6.58%, and 2.6% for the carbon steel, stainless steel, titanium, and aluminum, respectively. There are small differences between two methods for all materials.

Summarily, the errors of maximum stress and $x-$direction displacements between the M-PRBM and FEM are generated by calculated. The M-PRBM calculates the line while FEM base on the area. Moreover, materials change (elastic modulus E change) greatly affect the accuracy of the maximum stress and the $x-$direction displacement between M-PRBM and FEM. Therefore, M-PRBM theory is only suitable for materials with elastic modulus similar to aluminum material. Besides, when $h = 0.4$ mm and 0.5 mm, the error of maximum stress and the $x-$direction displacement increases as the material has an elastic modulus larger (i.e. the error is proportional to the elastic modulus E). However, when $h = 0.6$ mm, this error does

not change much when materials are changed, except for the average error of the maximum stress for titanium material.

5. Conclusions

In this paper, static analysis and optimization design are proposed for the fixed-guided beam flexures. These flexures are intended for driving the ratchet mechanism. The PRBM theory for large deformations of fixed-guided parallel beams flexures are used to calculate the maximum stress and the $x-$direction displacement. Predicted values from the analytical method are verified by FEM using ANSYS 18.1 software. The FEM simulations are established for three cases of the beams that have the height varying from 0.4 mm to 0.6 mm with four different materials. The configuration of the fixed-guided beam has been optimized for maximum $x-$direction displacement. Because there is a large error of maximum stress between PRBM and FEM, so M-PRBM is designed to obtain the accuracy of the maximum stress value. The value of $y-$direction displacement (parasitical displacement) is very small, so it is neglected. Compared with the FEM simulations, the M-PRBM is a better calculation of the maximum stress than the PRBM. The averaged errors between the M-PRBM and the FEM simulation are 3.48% for aluminum, and less than 10.9% for titanium, carbon steel, and alloy steel. The M-PRBM is therefore good for the design and fabrication of the compliant mechanism. Future work, the proposed method is extended for related compliant mechanisms.

Acknowledgement

This research is funded by Vietnam National Foundation for Science and Technology Development (NAFOSTED) under grant number 107.01-2019.14.

References

[1] Howell, L. L. (2001). Compliant mechanisms. Mechanical Engineering Department. Brigham Young University.

[2] Yuanqiang, L., & Wangyu, L. (2014). Analysis of the displacement of distributed compliant parallel-guiding mechanism considering parasitic rotation and deflection on the guiding plate. Mechanism and Machine Theory, 80, 151-165.

[3] Liu, Y., & Xu, Q. (2016). Design of a compliant constant force gripper mechanism based on buckled fixed-guided beam. In 2016 International Conference on Manipulation, Automation and Robotics at Small Scales (MARSS) (pp. 1-6). IEEE.

[4] Zhang, J., Yan, K., & Kou, Z. (2019). Design and Analysis of Flexible Hinge Used for Unfolding Spacecraft Solar Panels. Journal of Aerospace Technology and Management, 11.

[5] She, Y., Meng, D., Su, H. J., Song, S., & Wang, J. (2018). Introducing mass parameters to Pseudo–Rigid–Body models for precisely predicting dynamics of compliant mechanisms. Mechanism and Machine Theory, 126, 273-294.

[6] Mattson, C. A., Howell, L. L., & Magleby, S. P. (2004). Development of commercially viable compliant mechanisms using the pseudo-rigid-body model: case studies of parallel mechanisms. Journal of intelligent material systems and structures, 15(3), 195-202.

[7] Zirbel, S. A., Tolman, K. A., Trease, B. P., & Howell, L. L. (2016). Bistable mechanisms for space applications. PloS one, 11(12).

[8] Qi, K. Q., Ding, Y. L., Xiang, Y., Fang, C., & Zhang, Y. (2017). A novel 2-DOF compound compliant parallel guiding mechanism. Mechanism and Machine Theory, 117, 21-34.

[9] Liu, P., & Peng, Y. (2017). A modified pseudo-rigid-body modeling approach for

compliant mechanisms with fixed-guided beam flexures. Mechanical Sciences, 8(2), 359.

[10] Kennedy, J. A., Howell, L. L., & Greenwood, W. (2007). Compliant high-precision E-quintet ratcheting (CHEQR) mechanism for safety and arming devices. Precision engineering, 31(1), 13-21.

[11] Pei, X., Yu, J., Zong, G., & Bi, S. (2010). An effective pseudo-rigid-body method for beam-based compliant mechanisms. Precision Engineering, 34(3), 634-639.

[12] Dao, T. P., Ho, N. L., Nguyen, T. T., Le, H. G., Thang, P. T., Pham, H. T., Do, H. T., Tran, M. D., Nguyen, T. T. (2017). Analysis and optimization of a micro-displacement sensor for compliant microgripper. Microsystem Technologies, 23(12), 5375-5395.

[13] Lofroth, M., & Avci, E. (2019). Development of a novel modular compliant gripper for manipulation of micro objects. Micromachines, 10(5), 313.

[14] Gupta, V., Perathara, R., Chaurasiya, A. K., & Khatait, J. P. (2019). Design and analysis of a flexure based passive gripper. Precision Engineering, 56, 537-548.

[15] Chau, N. L., Dao, T. P., & Nguyen, V. T. T. (2018). Optimal design of a dragonfly-inspired compliant joint for camera positioning system of nanoindentation tester based on a hybrid integration of Jaya-ANFIS. Mathematical Problems in Engineering, 2018.

[16] Dang, M. P., Dao, T. P., Chau, N. L., & Le, H. G. (2019). Effective hybrid algorithm of Taguchi method, FEM, RSM, and teaching learning-based optimization for multiobjective optimization design of a compliant rotary positioning stage for nanoindentation tester. Mathematical Problems in Engineering, 2019.

[17] Le Chau, N., Le, H. G., & Dao, T. P. (2017). Robust parameter design and analysis of a leaf compliant joint for micropositioning systems. Arabian Journal for Science and Engineering, 42(11), 4811-4823.

[18] Reddy, J. N. (2006). Theory and analysis of elastic plates and shells. CRC press.

[19] Venkataraman, P. (2009). Applied optimization with MATLAB programming. John Wiley & Sons.

[20] Juvinall, R. C. and Marshek, K. M. (2017). Fundamentals of machine component. Professor of Mechanical Engineering. University of Michigan.

About Authors

Ngoc Thoai TRAN received his B.S. degree in mechanical engineering, Can Tho University, Vietnam, in 2009. He received his M.S. degree in mechanical engineering, Ho Chi Minh City University of Technology, in 2013. He is currently a lecturer at Faculty of Mechanical Engineering, Industrial University of Ho Chi Minh City, Vietnam. His research interests include compliant mechanism, assistive technology and rehabilitation, and optimization algorithm..

Thanh-Phong DAO is currently an assistant professor at the Institute for Computational Science, Ton Duc Thang University, Ho Chi Minh City, Vietnam. He received his B.S. degree in mechanical engineering from the Ho Chi Minh City University of Technology and Education, Vietnam in 2008. He received his M.S. and Ph.D. degree in mechanical engineering from the National Kaohsiung University of Applied Sciences, Taiwan, ROC, in 2011 and 2015, respectively. His research interests include compliant mechanism, assistive technology and rehabilitation, and optimization algorithm.